4th International Energy Conversion Engineering Conference and Exhibit (IECEC)
26 - 29 June 2006, San Diego, California

AIAA 2006-4141

Flow Structure Investigations in a "Tornado" Combustor

Igor Matveev[*]
Applied Plasma Technologies, Falls Church, Virginia, 22046

Serhiy Serbin[†]
National University of Shipbuilding, Mikolayiv, Ukraine, 54025

Thomas Butcher[‡]
Brookhaven National Laboratory, Upton, L.I., NY, 11973-5000

and

Narinder K. Tutu[§]
Brookhaven National Laboratory, Upton, L.I., NY, 11973-5000

A Reverse Vortex Combustor, in which aerodynamics dramatically differ from the conventional direct vortex combustor has been developed and preliminary testing has been done. A laser Doppler velocimetry system was used to measure the mean axial and swirl velocity components and their respective fluctuations in the "Tornado" combustor under cold, non-reacting, isothermal conditions. For modeling of the aerodynamical processes inside the combustor a generalized method was used based on numerical solution of the combined conservation and transport equations for turbulent system. Comparison between experimental data and computed predictions using different turbulence models has been completed.

I. Introduction

ENVIRONMENTAL and efficiency challenges and obstacles in using gaseous and liquid fuels, require modification of combustion processes, novel combustor designs, and the employment of low-emissions, effective flame stabilization devices. A new method of flame stabilization inside the reverse vortex flow provides the basis to build a prototype of the very effective combustion chamber named the "Tornado" combustor. Such a device, the aerodynamics of which dramatically differs from the conventional direct vortex combustor has been developed and preliminary tests have been completed, based on Applied Plasma Technologies (APT) recent patent applications[1-3]. Full-scale atmospheric pressure model tests proved the concept's advantages as follows[4]: highly efficient internal mixing of fuel and oxidizer, stable combustion with dramatically extended flammability limits, simple air swirler and fuel injectors, no necessity to cool the combustor walls, simple combustor design, cheaper materials for combustor fabrication, opportunity to feed fuel through the liner walls, and simple conversion into the multi-fuel and multi-zone combustor.

The main idea of the reverse-vortex stabilization is to establish a flame (or plasma jet) along the axis of a cylindrical combustion chamber in the opposite direction of the incoming air which is strongly swirling and flowing along the chamber walls. In this case, the cold gas cannot move to the inner, reverse flow zone before it loses the main part of its rotational speed. Hence, initially the cold gas flows along the wall to the closed end of the cylindrical vessel, and turbulent micro-volumes of this cold gas, which lost their kinetic energy near the wall, migrate radially towards the centre. As a result, the cold gas comes into the hot zone from all sides, except the outlet side, and no significant recirculation zone is formed.

---

[*] President & CEO, 7231 Woodley Place, Falls Church, VA 22046
[†] Professor, Dept. of Turbine Units, 9 Geroev Stalingrada Ave., Mikolayiv, Ukraine, 54025
[‡] Head of Energy Resources Division, Building 526, P.O. Box 5000, Upton, L.I., NY 11973-5000
[§] Mechanical Engineer, Energy Sciences and Technology Dept., Building 526, P.O. Box 5000, Upton, L.I., NY 11973-5000

Scaling efforts to evaluate advantages of this concept resulted in a Reverse Vortex Combustor (RVC)[4]. A complete atmospheric pressure combustor system, ID = 145 mm, internal volume of 4 liters (about one gallon) has been designed, manufactured and preliminary tests have been completed on natural gas with air flow up to 20 gram per second. It demonstrated extremely wide range of operation parameters with lean flameouts by 0.03, maximum wall temperature of about 240 °C at the exhaust gases temperature point of about 1400 °C.

While prototype combustion tests provided encouragement for this concept additional work is necessary to understand and optimize the combustion conditions. This has led to detailed study of a flow structure with the help of the laser Doppler technique. The Laser Doppler velocimetry (LDV) system is a widely accepted tool for fluid dynamic investigations in gases and liquids. It is a non-intrusive principle and directional sensitivity makes it very suitable for applications with reversing flow, chemically reacting or high-temperature media, where physical sensors are difficult or impossible to use. In this work, single-component laser Doppler velocimetry system was used to measure the mean axial and swirl velocity components and their respective fluctuations in the "Tornado" combustor. Due to the non-availability of a two-component LDV system, the axial and swirl velocity components could not be measured simultaneously. As a result, these were measured sequentially in different experimental runs under nominally identical conditions.

II. Mathematical Model

For modeling of physical processes inside the Tornado cold combustor a generalized method has been used, based on numerical solution of the combined conservation and transport equations for turbulent system[5-9]. This method provides a procedure of the sequential numerical integration of the 3D-differential equations that describe viscous gas flows.

The equation for conservation of mass, or continuity equation, can be written as follows:

$$\frac{\partial \rho}{\partial t} + \nabla \cdot (\rho \vec{v}) = S_m .$$

This equation is the general form of the mass conservation equation and is valid for incompressible as well as compressible flows. The source S_m is the mass added to the continuous phase from the dispersed second phase and any user-defined sources.

Conservation of momentum in an inertial reference frame is described by[5]:

$$\frac{\partial}{\partial t}(\rho \vec{v}) + \nabla \cdot (\rho \vec{v} \vec{v}) = -\nabla p + \nabla \cdot (\tau_{st}) + \rho \vec{g} + \vec{F} ,$$

where p is the static pressure, τ_{st} is the stress tensor, $\rho \vec{g}$ and $\vec{F}$ are the gravitational body force and external body forces, respectively. $\vec{F}$ contains other model-dependent source terms such as user-defined sources.

The stress tensor τ_{st} is given by

$$\tau_{st} = \mu[(\nabla \vec{v} + \nabla \vec{v}^T) - \frac{2}{3} \nabla \cdot \vec{v} I] ,$$

where μ is the molecular viscosity, I is the unit tensor, and the second term on the right hand side is the effect of volume dilation.

Additional transport equations are also solved when the flow is turbulent.

For cold aerodynamic prediction the RNG-based k-ε -turbulence model was used. This model is derived from the instantaneous Navier-Stokes equations, using a mathematical technique called "renormalization group" (RNG) methods[10]. The analytical derivation results in a model with constants different from those in the standard k-ε -model, and additional terms and functions in the transport equations for turbulence kinetic energy k and its dissipation rate ε.

Transport equations for the RNG k-ε-model have a similar form to the standard k-ε-model:

$$\frac{\partial}{\partial t}(\rho k)+\frac{\partial}{\partial x_i}(\rho k u_i)=\frac{\partial}{\partial x_j}(\alpha_k \mu_{eff}\frac{\partial k}{\partial x_j})+G_k+G_b-\rho\varepsilon-Y_M+S_k$$

$$\frac{\partial}{\partial t}(\rho \varepsilon)+\frac{\partial}{\partial x_i}(\rho \varepsilon u_i)=\frac{\partial}{\partial x_j}(\alpha_\varepsilon \mu_{eff}\frac{\partial \varepsilon}{\partial x_j})+C_{1\varepsilon}\frac{\varepsilon}{k}(G_k+C_{3\varepsilon}G_b)-C_{2\varepsilon}\rho\frac{\varepsilon^2}{k}-R_\varepsilon+S_\varepsilon$$

In these equations, G_k represents the generation of turbulence kinetic energy due to the mean velocity gradients, G_b is the generation of turbulence kinetic energy due to buoyancy, Y_M represents the contribution of the fluctuating dilatation in compressible turbulence to the overall dissipation rate. The quantities α_k and α_ε are the inverse effective Prandtl numbers for *k* and ε, respectively, and S_k and S_ε are user-defined source terms.

The main difference between the RNG and standard *k*-ε -models lies in the additional term in the ε equation given by

$$R_\varepsilon=\frac{C_\mu \rho \eta^3(1-\eta/\eta_0)}{1+\beta\eta^3}\frac{\varepsilon^2}{k},$$

where $\eta = Sk/\varepsilon$, $\eta_0 = 4.38$, $\beta = 0.012$.

The scale elimination procedure in the RNG theory results in a differential equation for turbulent viscosity:

$$d(\frac{\rho^2 k}{\sqrt{\varepsilon\mu}})=1.72\frac{\hat{\nu}}{\sqrt{\hat{\nu}^3-1+C_\nu}}d\hat{\nu},$$

where

$$\nu=\mu_{eff}/\mu,\ C_\nu \approx 100.$$

This equation is integrated to obtain an accurate description of how the effective turbulent transport varies with the effective Reynolds number (or eddy scale), allowing the model to better handle low-Reynolds-number and near-wall flows.

Turbulence, in general, is affected by rotation or swirl in the mean flow. The RNG model provides an option to account for the effects of swirl or rotation by modifying the turbulent viscosity appropriately. The modification takes the following functional form:

$$\mu_t=\mu_{t0}f(\alpha_s,\Omega,\frac{k}{\varepsilon}),$$

where μ_{t0} is the value of turbulent viscosity calculated without the swirl modification. Ω is a characteristic swirl number, and α_s is a swirl constant that assumes different values depending on whether the flow is swirl-dominated or only mildly swirling.

In comparison with the standard *k*-ε -model, the smaller destruction of ε augments, reducing *k* and, eventually, the effective viscosity. As a result, in rapidly strained flows, the RNG model yields a lower turbulent viscosity than the standard *k*-ε -model. Thus, the RNG model is more responsive to the effects of rapid strain and streamline curvature than the standard *k*-ε -model, which explains the superior performance of the RNG model for certain classes of flows.

Turbulent flows in "Tornado" combustor are characterized by eddies with a wide range of length and time scales. The largest eddies are typically comparable in size to the characteristic length of the mean flow. The smallest scales are responsible for the dissipation of turbulence kinetic energy. Therefore in some cases for definition of instantaneous velocities inside "Tornado" and its comparison with LDV data the large eddy simulation (LES) model has been used.

It is assumed that momentum, mass, energy, and other passive scalars are transported mostly by large eddies. Large eddies are more problem-dependent; small eddies are less dependent on the geometry, tend to be more isotropic, and are consequently more universal.

A filtered variable (denoted by an overbar) is defined by

$$\bar{\phi}(x) = \int_D \phi(x')G(x, x')dx'$$

where D is the fluid domain, and G is the filter function that determines the scale of the resolved eddies.

Filtering the Navier-Stokes equations for LES modeling can be written in the following form

$$\frac{\partial \rho}{\partial t} + \frac{\partial}{\partial x_i}(\rho \bar{u}_i) = 0 ,$$

$$\frac{\partial}{\partial t}(\rho \bar{u}_i) + \frac{\partial}{\partial x_j}(\rho \bar{u}_i \bar{u}_j) = \frac{\partial}{\partial x_j}(\mu \frac{\partial \sigma_{ij}}{\partial x_j}) - \frac{\partial \bar{p}}{\partial x_i} - \frac{\partial \tau_{ij}}{\partial x_j} ,$$

where σ_{ij} is the stress tensor due to molecular viscosity defined by

$$\sigma_{ij} = [\mu(\frac{\partial \bar{u}_i}{\partial x_j} + \frac{\partial \bar{u}_j}{\partial x_i})] - \frac{2}{3}\mu \frac{\partial \bar{u}_l}{\partial x_l}\delta_{ij} ,$$

and τ_{ij} is the subgrid-scale stress defined by

$$\tau_{ij} = \rho \overline{u_i u_j} - \rho \bar{u}_i \bar{u}_j .$$

The subgrid-scale stresses resulting from the filtering operation are unknown, and require modeling. The subgrid-scale turbulence models employ the Boussinesq hypothesis[11] as in the RANS models, computing subgrid-scale turbulent stresses from

$$\tau_{ij} - \frac{1}{3}\tau_{kk}\delta_{ij} = -2\mu_t \bar{S}_{ij} ,$$

where μ_t is the subgrid-scale turbulent viscosity, and $\bar{S}_{ij}$ is the rate-of-strain tensor for the resolved scale defined by

$$\bar{S}_{ij} = \frac{1}{2}(\frac{\partial \bar{u}_i}{\partial x_j} + \frac{\partial \bar{u}_j}{\partial x_i}) .$$

For μ_t determination the dynamic Smagorinsky-Lilly[12-14] model was used. In this model, the eddy-viscosity is modeled by

$$\mu_t = \rho L_S^2 |\bar{S}| ,$$

where L_S is the mixing length for subgrid scales, and $|\bar{S}| = \sqrt{2\bar{S}_{ij}\bar{S}_{ij}}$.

L_S is computed using

$$L_S = \min(\mathrm{K}d, C_S V^{1/3})$$

where K is the von Karman constant, d is the distance to the closest wall, C_S is the Smagorinsky constant, and V is the volume of the computational cell.

In the dynamic Smagorinsky-Lilly[15] model constant, C_S, is dynamically computed based on the information provided by the resolved scales of motion. The C_S obtained using the dynamic Smagorinsky-Lilly model varies in time and space over a fairly wide range.

The boundary conditions in the axial and tangential inlets, symmetry axes, walls and outlet from a RVC were set in accordance with the conditions for carrying out physical experiments and recommendations for modeling the turbulent processes. The method for the system solution, the finite difference scheme and the solution stability analysis are explained in references[9-15].

III. Experimental Setup for the LDV Measurements

A full-scale atmospheric pressure model of the "Tornado" combustor has length of 240 mm. Air comes into combustor through the swirler with tangential channels, located in the area of the exit port, the diameter of which was varied from 62 to 102 mm in the experiments. The flexible combustor design provided fast and simple replacement of the carbon steel shell with quartz tubing for the LDV process visualization.

Since the laser Doppler technique uses the scattered light from particles in the flow to measure the flow velocities, particles need to be injected into the flow. A commercial "fluidized bed particle generator" was used for this purpose to inject titanium dioxide particles in the air stream of the "Tornado" combustor. The LDV system consists of the following components: Laser, Detector, and Optics Module (designated in the text by "LDV probe"), and Digital Burst Processor (Fig. 1-2).

The laser has a wavelength of 685 nm and a power of 50 mW (25 mW for each of the two beams). The Burst Processor contains the electronics to process the signals from the LDV probe. It is controlled from a desktop personal computer (PC) via commercial LDV software, and the processed data is transferred to the PC. A 350-mm focal length lens is connected to the front end of the LDV probe. It outputs two laser beams that are 50 mm apart at the exit of the lens. To enable the measurement of the direction of the velocity component, the frequency of one of the beams is shifted by 40 MHz by the Bragg cell in its path. The measurement volume (the location at which the instantaneous velocity is measured) formed by the region of intersection of the two laser beams is an elongated ellipsoid 3.8-mm in length with minor axes of 0.3 mm and 0.1 mm.

For all the measurements performed, the 3.8-mm long major axis was always aligned parallel to the radial direction (Fig. 3). The velocity data from a given location consists of a series of instantaneous values: u_1, u_2, …, u_n, which are recorded at discrete times t_1, t_2, …, t_n. These data can then be used to calculate such items as the

Figure 1. Experimental setup showing the plasma chamber, the LDV probe, the particle generator, and the traversing mechanism.

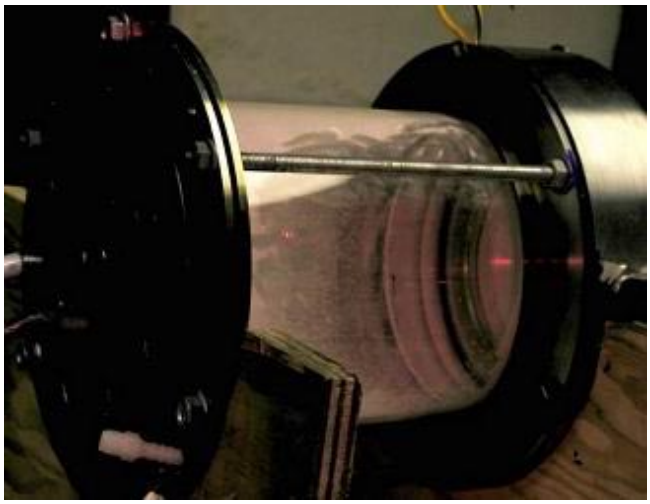

Figure 2. A close-up of the plasma chamber with the laser beam on.

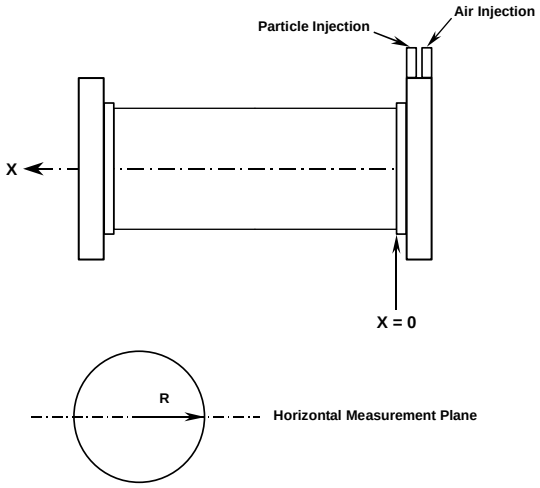

Figure 3. Definition sketch for coordinate system at air flow rate 2.15 g/s.

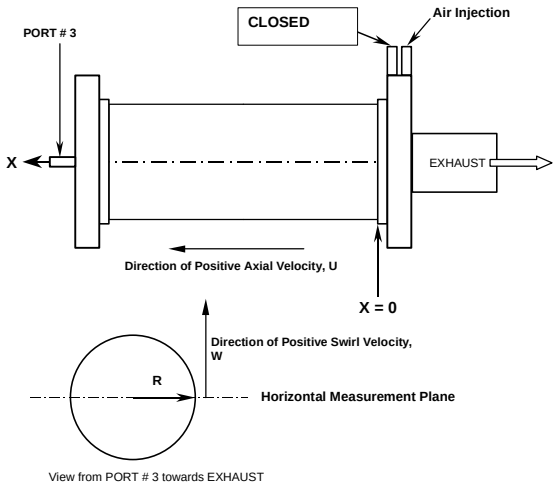

Figure 4. Definition sketch for coordinate system at air flow rate 8.1 g/s.

time-averaged mean velocity, the root mean square velocity fluctuation, and the probability density function of the velocity component.

During low-flow LDV measurements (Fig. 3) air from the blower was injected at the normal "air inlet port". Particles were injected from the "fuel inlet port". The air flow rate through the particle injection port is 17 standard liters per minute for all cases. The static pressure at the air inlet port due to the blower was 4 inches of water, that corresponds to an inlet air flow rate of 2.15 g/s. Even at very low flow rates, a vortex flow inside the quartz chamber has been observed. . In this geometry a flow rate of less than 1 cfm seems to be enough to establish a vortex flow.

During high-flow LDV measurements (Fig. 4) air from the blower was injected at the normal "air inlet port". Particles were injected from the "fuel inlet port # 3". This port is along the centerline. The air flow rate through the particle injection port is 16 standard liters per minute for all cases. The static pressure at the air inlet port due to the blower was 2 psig, that corresponds to an inlet air flow rate of 8.1 g/s.

IV. Comparison Between Experimental and Calculated Data

The flow structure features inside the Tornado Combustor for cold flow under both low and high flow using the LDV system have been studied. The distributions of the mean axial and swirl velocity components and their fluctuations at three combustor cross-sections (X = 5, 50 and 110 mm from the beginning of optical section as indicated in Figures 3 and 4) have been obtained. According to the experimental data, the velocity component distribution on the chamber radius is non-uniform. For input to the CFD computations the calculations of the inlet ring channel with four tangential air orifices have been previously conducted and the resulting air flow rate distribution through individual orifices was determined.

A. Flow Structure Investigation at Low Air Flow Conditions

Experimental measurements of mean velocities and RMS of velocity fluctuations are averages over a time period of 300 seconds. Thus they represent the influences over eddies sizes ranging from small scales to large scales.

In most cases for aerodynamics "Tornado" prediction RNG k-ε-turbulence steady state model with swirl dominated flow, segregated solver for steady formulation, SIMPLE method for pressure-velocity coupling, and second order upwind discretization scheme for density, momentum, turbulence kinetic energy, turbulence dissipation rate and energy were used.

Contours of the CFD-predicted mean axial velocity, turbulence kinetic energy, and velocity vectors near the combustor exit region are shown in Fig. 5. It is obvious that the presence of a vortex system inside the "Tornado" combustor causes the recirculating flow at the nozzle exit region. The velocity contours at the chamber exit are extremely non uniform thereby causing large shears in air flow.

Experimental and calculated mean axial and swirl velocities distribution at the X distance of 25, 50 and 115 mm are shown in Fig. 6-7. Using both the steady RNG k-ε-model and transient LES calculations gives good quantitative conformity with experimental data. Note, that for Large Eddy Simulation we used: Smagorinsky-Lilly dynamic

model, discretization: density – second order upwind, momentum – bounded central differencing, energy – second order upwind, and pressure-velocity coupling – SIMPLEC.

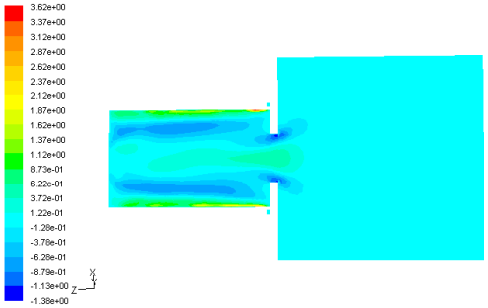

a)

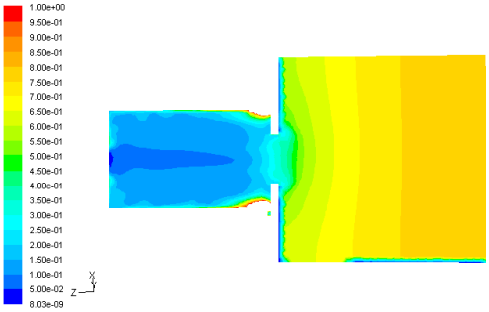

b)

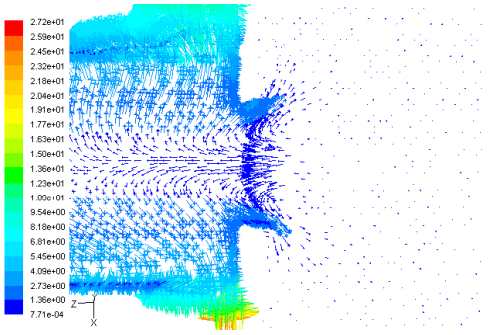

c)

Figure 5. Contours of mean axial velocities (a), m/s, turbulence kinetic energy (b), m^2/s^2, and velocity vectors (c) at combustor exit region, m/s.

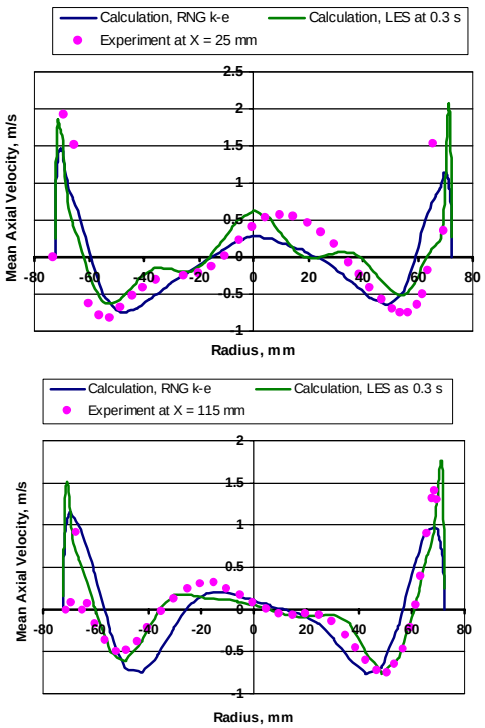

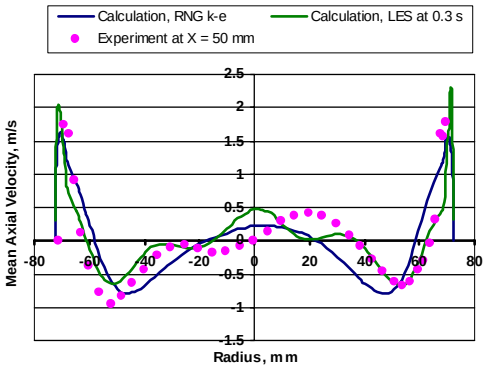

Figure 6. Experimental and calculated mean axial velocities distribution.

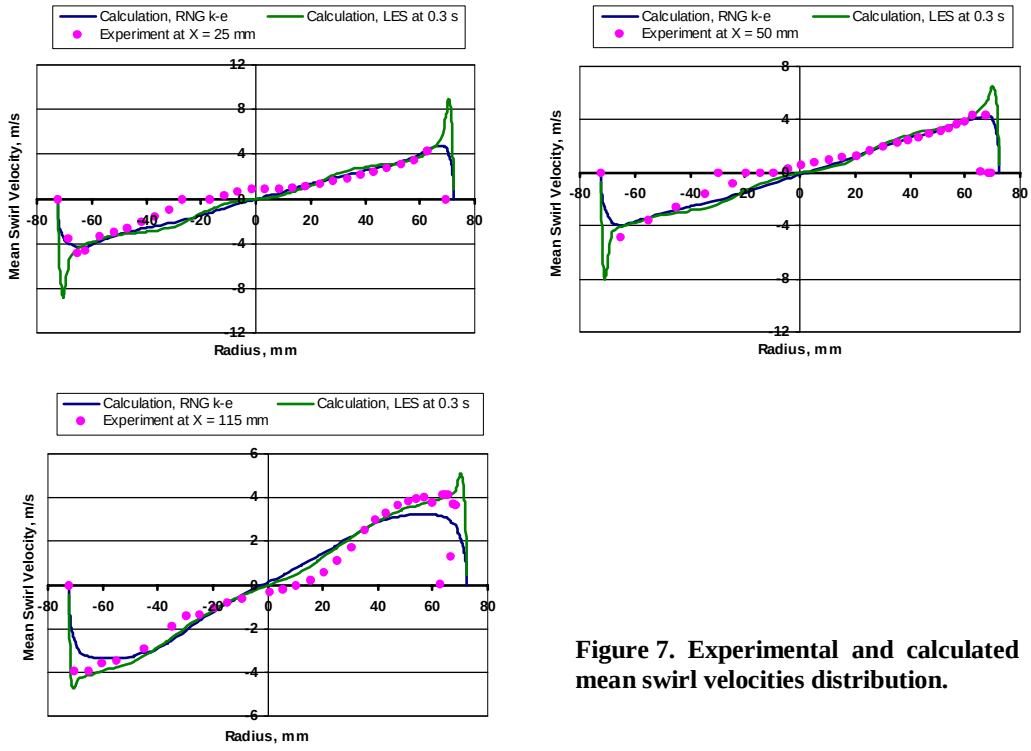

Figure 7. Experimental and calculated mean swirl velocities distribution.

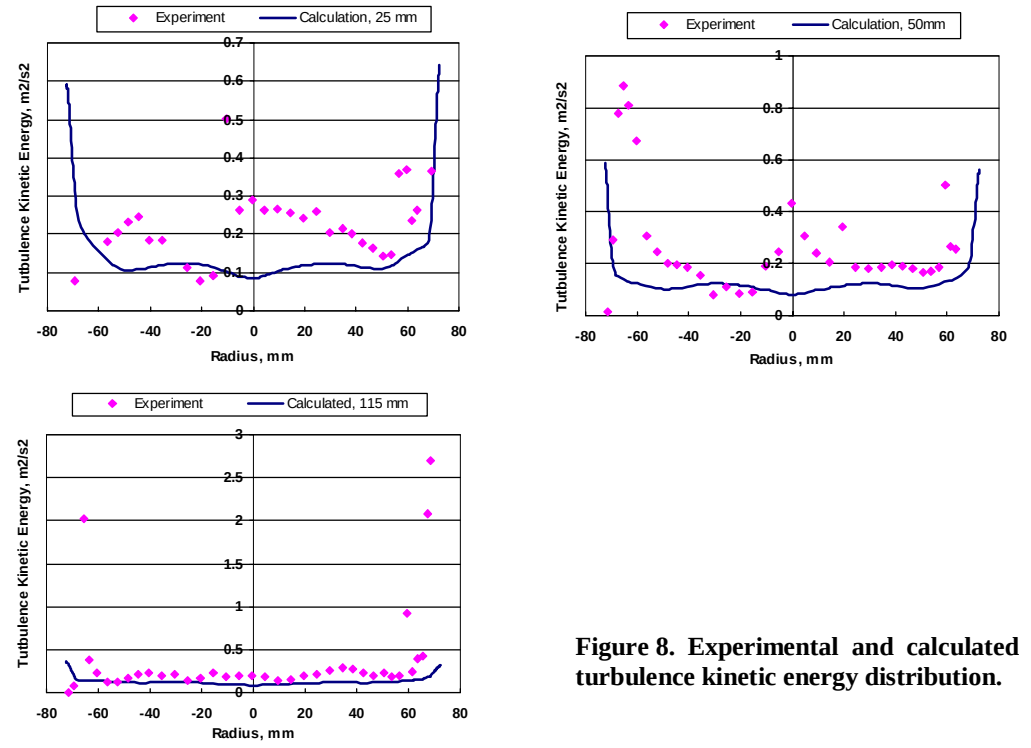

Figure 8. Experimental and calculated turbulence kinetic energy distribution.

The experimental profile of mean swirl velocity for the low flow rate case has a large region with zero mean swirl velocity, indicating that the vortex is oscillating radially. It causes instability in the vortex position inside the combustor, and large difficulties for mathematical modeling of turbulent fluctuation parameters.

The experimental turbulence kinetic energy can be calculated as

$$k = \frac{1}{2}(u'^2 + v'^2 + w'^2),$$

therefore there is the possibility to compare the k from CFD steady RNG k-ε-model predictions to measured k.

Since during the experiments the v' fluctuations were not measured, and since the measurements have shown that the magnitudes of u' and w' are of the same order, we assumed that $v' = (u' + w')/2$, and then calculated the experimental k.

Since the vortex centerline is oscillating radially at the low flow rate of 2.15 g/s (as inferred from the LDV experimental data on Fig. 7), this will contribute to larger velocity fluctuations (u', and w') as compared to the case in which the vortex axis is stable. Since for the CFD case the vortex centerline is fixed at radius r = 0, one would expect the measured k to be higher than the steady state k predicted by CFD. This fact agrees with data in Fig. 8, where comparison between experimental and calculated turbulence kinetic energy profiles is illustrated.

It is interesting to examine the velocity fluctuation variations inside the "Tornado" combustor. In Figs. 9-10, comparisons between experimental and calculated RMS fluctuations in axial and swirl velocities are presented.

LES provides the approach in which large eddies are explicitly computed in a time-dependent simulation using the "filtered" Navier-Stokes equations. Therefore only larger eddies need be resolved. Statistics of the time-varying flow fields such as time-averages and RMS values of the velocity components can be collected during the transient simulation. Note, that the use of dynamic Smagorinsky-Lilly model assumes local equilibrium of sub-grid scales, scale similarity between the smallest resolved scales and the sub-grid scales.

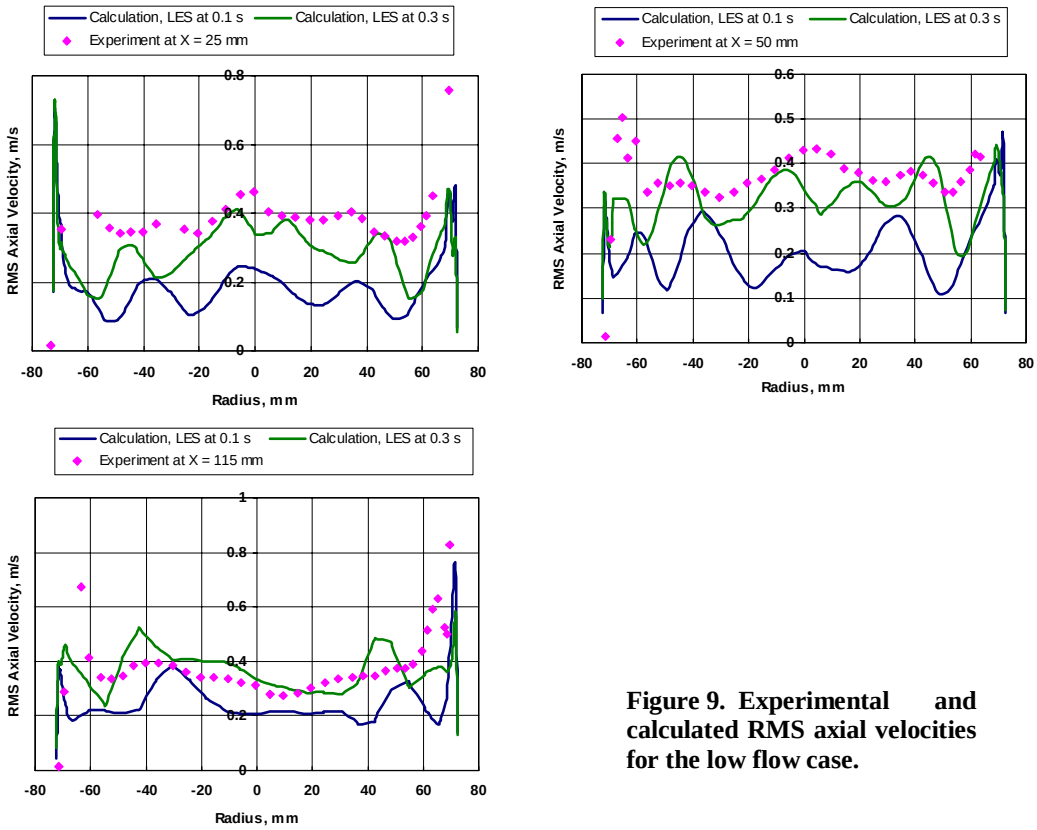

Figure 9. Experimental and calculated RMS axial velocities for the low flow case.

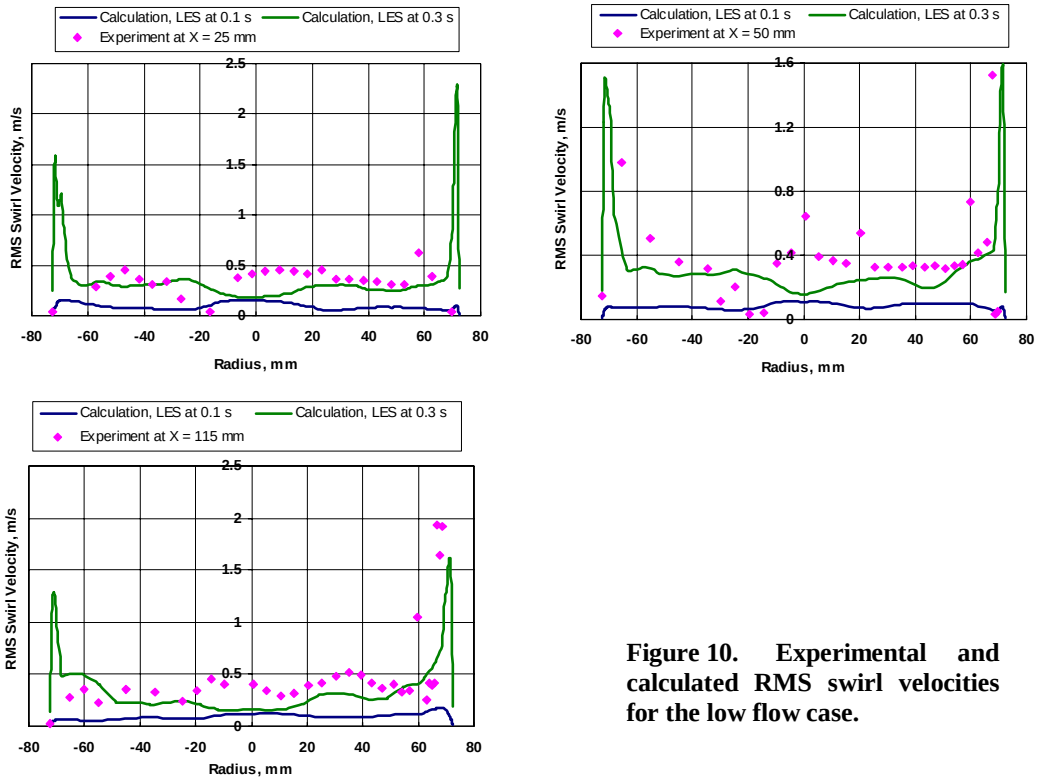

Figure 10. Experimental and calculated RMS swirl velocities for the low flow case.

If r is the combustor chamber radius (r = 72.5 mm), W_{max} is the peak mean swirl velocity slightly away from the wall, and t is the time a fluid particle will take for one revolution, then $2\pi r \approx tW_{max}$. For air flow rate of 2.15 g/s, W_{max} is around 4 m/s and. This gives approximately t = 0.11 seconds. Therefore CFD LES simulation time of 0.3 seconds corresponds to about 3 revolutions of the vortex, and 0.1 second corresponds to less than 1 revolution of the air vortex. This explains why the results for the RMS axial and swirl velocity fluctuations for 0.3 seconds-calculation period are so much better than that for the calculation period of 0.1seconds. Since the vortex is moving radially, in order to get reasonable values of RMS velocity fluctuations, it is necessary that the total simulation time be equal to at least several rotational cycles.

B. Flow Structure Investigation at High Air Flow Conditions

For steady and transient aerodynamics "Tornado" combustor prediction at the high air flow conditions (8.1 g/s) the RNG k-ε-turbulence model with swirl dominated flow, and Large Eddy Simulation with Smagorinsky-Lilly dynamic model were used.

Note that due to the lack of data close to the combustor walls, there are very few (or no) measurements in the regions where one expects large positive velocities.

Experimental and calculated (using steady RNG k-ε-model) mean axial and swirl velocities on a X distance of 50 and 115 mm are presented in Fig. 11-12. CFD calculations give more extensive inverse flow at paraxial exit nozzle area in comparison with experiment.

As shown by the swirl velocity component distributions in Fig. 12, note that for the high flow rate case, the central air vortex is better defined.

Experimental and calculated RMS axial velocities are shown in Fig. 13. The measured and predicted values are of the same order of magnitude. This is a measure of the qualitative reliability of the mathematical turbulence model for the Tornado Combustor.

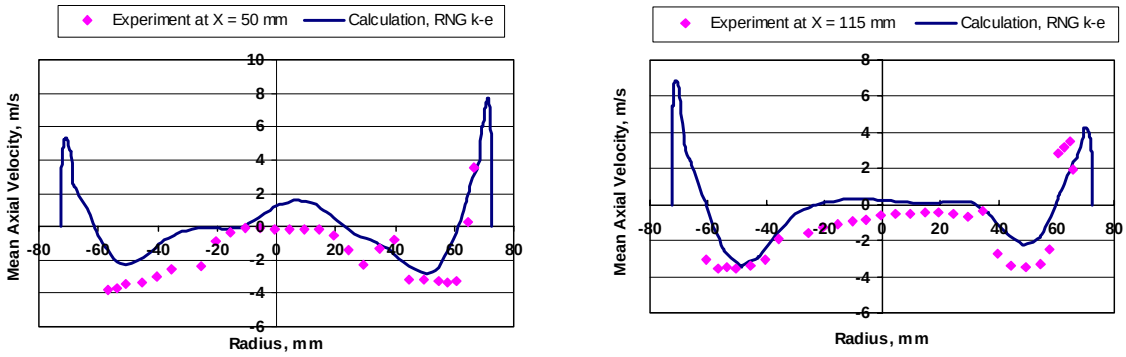

Figure 11. Experimental and calculated mean axial velocities for the high flow case.

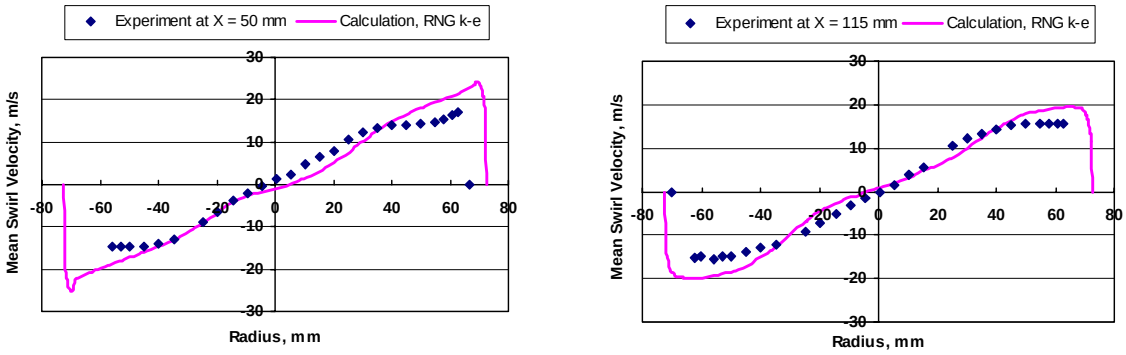

Figure 12. Experimental and calculated mean swirl velocities for the high flow case.

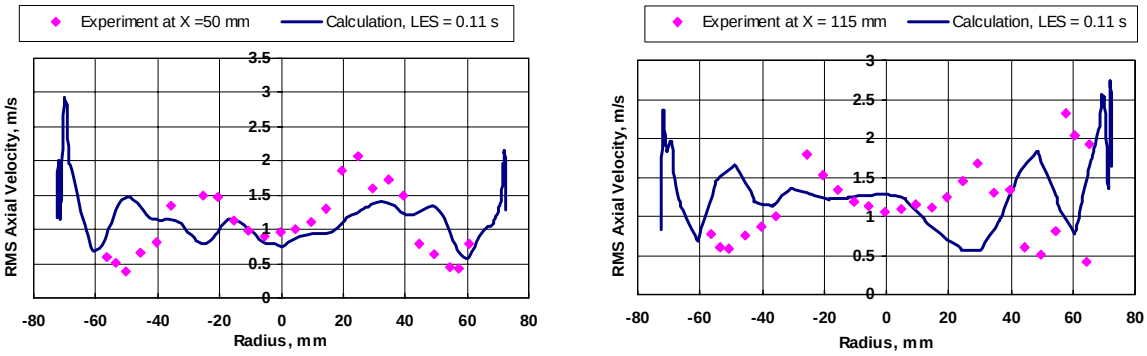

Figure 13. Experimental and calculated RMS axial velocity fluctuations.

C. Probability Density Function (PDF) of the Instantaneous Axial and Swirl Velocity Components

In Figs. 14-15 experimental probability density functions of the instantaneous axial and swirl velocities are presented. Note that $P(U)dU$ is the probability that the instantaneous axial velocity component lies between U and $(U+dU)$, and $P(W)dW$ is the probability that the instantaneous swirl velocity component lies between W and $(W+dW)$. These figures show very different character of axial and swirl velocities fluctuations near the centerline at low and high air flow conditions. At low flow conditions the PDFs are trimodal indicating that the vortex centerline is fluctuating radially.

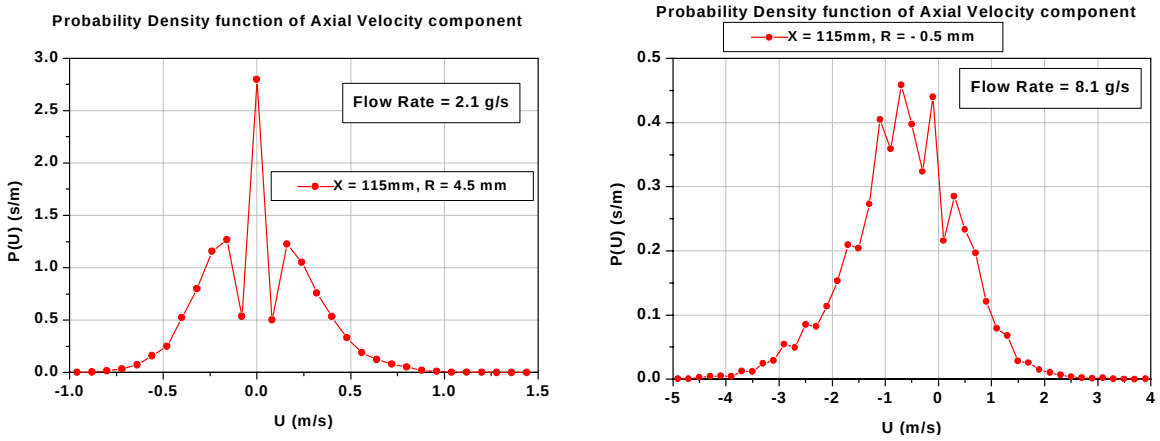

Figure 14. Probability density function of the instantaneous axial velocity component near the centerline at X = 115 mm for the low and high flow rate cases.

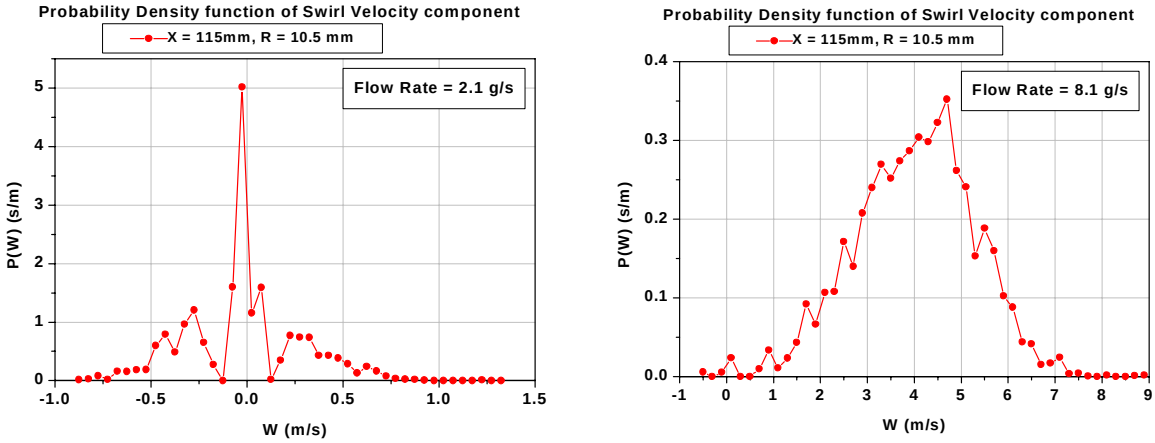

Figure 15. Probability density function of the instantaneous swirl velocity component near the centerline at X = 115 mm for the low and high flow rate cases.

V. Conclusion

We have conducted experimental and theoretical investigations demonstrating the modeling opportunity for the complex aerodynamic flows without chemical reactions in the "Tornado" reverse vortex combustor. This exercise has revealed the weak sides of the existing turbulence models and has also shown the main directions for improving the mathematical model. If further funding for this work becomes available, we plan to extend the experimental and CFD simulations to the case of a Tornado Combustor with combustion (reacting non-isothermal flow).

Acknowledgments

The authors would like to acknowledge Dr. Alexander Gutsol from Drexel University for his introduction into the reverse vortex flow investigations and Anna Mostipanenko from National University of Shipbuilding, Ukraine, for her mesh preparation and CFD calculations.

References

[1]Matveev, I., US Patent Application # 60/602,185 for a "Reverse Vortex Reactor with Spatial Arc", filed 17 August 2004.

[2]Matveev, I., Gutsol, A., US Patent Application # 60/617,861 for a "Reverse Vortex Combustion Chamber", filed 13, October 2004.

[3]Matveev, I., US Patent Application for a "Plasma Assisted Combustion System", filed 24, December 2004.

[4]Matveev, I., Serbin, S., "Experimental and Numerical Definition of the Reverse Vortex Combustor Parameters", *44th AIAA Aerospace Sciences Meeting and Exhibit* AIAA 2006-551, Reno, Nevada, 2006, pp. 1-12.

[5]Batchelor, G. K., *An Introduction to Fluid Dynamics*, Cambridge Univ. Press, Cambridge, England, 1967.

[6]Launder B. E., Spalding D. B., *Lectures in Mathematical Models of Turbulence*. Academic Press, London, 1972.

[7]Jones W.P., Priddin C.H.,"Predictions of the Flow Field and Local Gas Composition in Gas Turbine Combustors", *Seventeenth Symp. (Int.) on Combustion*, Pittsburgh, 1978, pp. 399-409.

[8]Mador R.J., Roberts R. A., "Pollutant Emissions Prediction Model for Gas Turbine Combustors", *AIAA Paper*, 1978, No. 998, pp. 1-14.

[9]Serbin S.I., "Modeling and Experimental Study of Operation Process in a Gas Turbine Combustor with a Plasma-Chemical Element", *Combustion Science and Technology*, Vol. 139, 1998.

[10]Choudhury, D., "Introduction to the Renormalization Group Method and Turbulence Modeling", Fluent Inc. Technical Memorandum TM-107, 1993.

[11]Hinze, J. O., *Turbulence*, McGraw-Hill Publishing Co., New York, 1975.

[12]Smagorinsky, J., "General Circulation Experiments with the Primitive Equations. I. The Basic Experiment", *Month. Wea. Rev*., 91:99-164, 1963.

[13]Germano, M., Piomelli, U., Moin, P., and Cabot, W. H., "Dynamic Subgrid-Scale Eddy Viscosity Model", *Summer Workshop, Center for Turbulence Research*, Stanford, CA, 1996.

[14]Lilly, D. K., "A Proposed Modification of the Germano Subgrid-Scale Closure Model", *Physics of Fluids*, 4:633-635, 1992.

[15]Kim, S. E., "Large eddy simulation using unstructured meshes and dynamic subgrid-scale turbulence models", Technical Report AIAA-2004-2548, 2004.